OPEN

# Emodin Alleviates Sodium Taurocholate–Induced Pancreatic Ductal Cell Damage by Inhibiting the S100A9/VNN1 Signaling Pathway

*Fangyue Guo, PhD,*† Qi Zhou, PhD,*† Yu Wu, MS,‡§ Mingming Chen, MS,‡§ Liang Zhao, MD,|| and Hong Xiang, PhD**

**Objectives:** Because the pathogenesis of the disease is unclear, the treatment of patients with acute pancreatitis, especially severe acute pancreatitis, is still a major challenge for clinicians. Emodin is an anthraquinone compound extracted from rhubarb that can alleviate the damage to pancreatic ductal epithelial cells induced by adenosine triphosphate, but whether it has a similar protective effect on sodium taurocholate (STC)–stimulated pancreatic ductal cells and the underlying mechanism has not yet been reported.

**Methods:** A model of STC-induced HPDE6-C7 human pancreatic ductal epithelial cell injury was established, and then apoptosis and the levels of reactive oxygen species (ROS), glutathione, gamma-glutamylcysteine synthetase, and inflammatory cytokines were assessed in the presence or absence of emodin pretreatment. S100 calcium binding protein A9 (S100A9) and Vanin1 (VNN1) protein expression was also measured.

**Results:** Emodin significantly increased HPDE6-C7 cell viability, inhibited apoptosis and ROS release, and elevated glutathione levels and gamma-glutamylcysteine synthetase activity. Furthermore, emodin downregulated S100A9 and VNN1 protein expression and inhibited the production of inflammatory factors, such as interleukin (IL)-1β, IL-6, IL-8, and IL-18.

**Conclusions:** Emodin attenuates STC-induced pancreatic ductal cell injury possibly by inhibiting S100A9/VNN1-mediated ROS release. This finding provides evidence for the future development of emodin as a therapeutic agent.

**Key Words:** acute pancreatitis, ductal cells, emodin, S100 calcium binding protein A9, Vanin1

(*Pancreas* 2022;51: 739–746)

From the *Laboratory of Integrative Medicine, First Affiliated Hospital of Dalian Medical University; †Institute (College) of Integrative Medicine, Dalian Medical University; ‡Department of Clinical Pharmacy, First Affiliated Hospital of Dalian Medical University; §College of Pharmacy, Dalian Medical University; and ||Department of General Surgery, First Affiliated Hospital of Dalian Medical University, Dalian, China.

Received for publication July 5, 2021; accepted August 2, 2022.

Address correspondence to: Liang Zhao, MD, Department of General Surgery, First Affiliated Hospital of Dalian Medical University, No. 222 Zhongshan Road, Dalian 116011, China (e-mail: zhaoliangeagle@163.com); or Hong Xiang, PhD, Laboratory of Integrative Medicine, First Affiliated Hospital of Dalian Medical University, No. 222 Zhongshan Road, Dalian, 116011, China (e-mail: xianghong@dmu.edu.cn).

This work was supported by grants from the Scientific Research Project of Department of Education of Liaoning Province (no. LZ2020075) and the Scientific Research Project of Traditional Chinese Medicine of Dalian (no. 20Z12003).

F.G. and Q.Z. performed the experiments and drafted the manuscript. Y.W. and M.C. assisted performing western blotting and quantitative real-time polymerase chain reaction. L.Z. and H.X. conceived and designed the experiments.

The authors declare no conflict of interest.

Copyright © 2022 The Author(s). Published by Wolters Kluwer Health, Inc. This is an open-access article distributed under the terms of the Creative Commons Attribution-Non Commercial-No Derivatives License 4.0 (CCBY-NC-ND), where it is permissible to download and share the work provided it is properly cited. The work cannot be changed in any way or used commercially without permission from the journal.

DOI: 10.1097/MPA.0000000000002098

Acute pancreatitis (AP), defined as the rapid onset of pancreatic inflammation, is the most common gastrointestinal disease leading to hospital admission worldwide.[1] The annual incidence of AP ranges from 13 to 45 per 100,000 individuals in the United States, and the mortality rate of severe AP (comprising approximately 10% of all cases) remains remarkably high (~28%).[2,3] The typical characteristics of AP are acinar cell injury and exocrine abnormalities, and sustained inflammation is responsible for local or systemic inflammatory response syndrome.[4,5] Thus, most studies have focused on pancreatic acinar cell damage mediated by various stimuli and its underlying molecular mechanisms.[6–8] The exocrine pancreas is composed of both acinar and ductal cells. These 2 types of exocrine cells interact closely to maintain the normal physiological function of the pancreas.[9] Pancreatic acinar cell destruction is undoubtedly the terminal step in pancreatitis, but the duct plays a crucial role in maintaining the integrity of the pancreas; when this protective function is compromised, pancreatitis occurs.[10,11] Under physiological conditions, the primary function of the pancreatic duct is to secrete ductal fluid and $HCO_3^-$, which together form a ductal mucosal barrier that protects the pancreas from noxious stimuli by blocking the backflow of bile and trypsin into the pancreas.[12] Previous studies have shown that high concentrations of bile acids inhibit $HCO_3^-$ secretion, thus leading to damage to the epithelial barrier. The ducts can no longer protect against bile acids, and loss of this protective effect may contribute to the progression of AP.[10] Given the anatomy and biological functions of the pancreatic duct, the pancreatic ductal epithelium seems to be vulnerable to harmful stimuli, such as endoscopic retrograde pancreatography and gallstone passing.[13,14] However, the mechanisms of pancreatic duct injury in AP pathogenesis have not been clarified, and further exploration is warranted.

S100 calcium binding protein A9 (S100A9), also known as myeloid-related protein-14, is one of the primary members of the S100 protein family and has been demonstrated to play an important role in the regulation of migration or adherence of inflammatory cells.[15] Our previous study showed that deletion of S100A9 in the pancreatic duct ameliorates AP by targeting Vanin1 (VNN1)-mediated reactive oxygen species (ROS) release, which provides evidence for S100A9 as a potential therapeutic target for AP.[16]

The Chinese herb rhubarb has been used alone or as a monarch herb in traditional Chinese medicine (TCM) formulas (eg, Qingyi decoction, Dachengqi decoction, and Yinchenhao decoction) to treat AP for many years.[17–20] Emodin (1,3,8-trihydroxy-6-methylanthraquinone) is an anthraquinone derivative mainly extracted from rhubarb and has effects against AP in vitro and in vivo.[21,22] Recent studies on the effect of emodin against AP have focused mainly on its ability to protect pancreatic acinar cells and suppress the inflammatory cascade.[23,24] Interestingly, our previous research found that emodin also ameliorates the damage to pancreatic ductal epithelial cells induced by adenosine triphosphate in vitro.[25] In this article, a model of sodium taurocholate (STC)–induced damage was first established to explore the protective effect of emodin

against pancreatic duct injury in vitro. Emodin may alleviate STC-induced pancreatic ductal epithelial cell damage by inhibiting apoptosis and inflammation by targeting the S100A9/VNN1 pathway.

## MATERIALS AND METHODS

### Reagents and Materials

High-glucose Dulbecco's modified Eagle's medium was obtained from HyClone Co (Logan, Utah). Fetal bovine serum, trypsin-Ethylene Diamine Tetraacetic Acid (0.05%), and phenol red were provided by Gibco Co, Ltd (Thermo Fisher Scientific, Cleveland, Ohio). Emodin and STC were purchased from Solarbio Science and Technology Co (Beijing, China). PrimeScript RT reagent and SYBR PremixEx Taq II (TliRNaseH Plus) were purchased from TaKaRa Biotechnology Co, Ltd (Dalian, China). RNAex Pro RNA reagent was obtained from Accurate Biology Co, Ltd (Changsha, China). A ROS Detection Assay Kit was purchased from AmyJet Scientific Inc Co, Ltd (Wuhan, China). An α-Amylase (α-AMS) Assay Kit and Gamma-Glutamylcysteine Synthetase (γ-GCS) Assay Kit were provided by the Nanjing Jiancheng Institute of Biotechnology (Nanjing, China). A Micro Reduced Glutathione (GSH) Assay Kit was provided by Solarbio Science and Technology Co (Beijing, China). Rabbit anti-S100A9 was purchased from Cell Signaling Technology, Inc (Beverly, Mass). Rabbit anti-VNN1 was purchased from the Proteintech Group (Chicago, Ill). Goat antirabbit IgG H&L (Horseradish Peroxidase) was obtained from Abcam (Cambridge, UK). An Annexin V-FITC/PI Apoptosis Detection Kit was provided by Dalian Meilun Biotechnology Co, Ltd (Dalian, China).

### Cell Culture

The HPDE6-C7 human pancreatic duct cell line was obtained from American Type Culture Collection (Manassas, Va). The cells were cultured in high-glucose Dulbecco's modified Eagle medium supplemented with 10% fetal bovine serum in a humid environment containing 5% $CO_2$ at 37°C.

### Cell Viability Assay

A cell viability assay was used to determine the cytotoxicity of emodin and the optimum concentration and duration of emodin treatment. Emodin was dissolved in dimethyl sulfoxide before being added to cells; the final concentration of dimethyl sulfoxide was less than 0.1%. Briefly, HPDE6-C7 cells were plated in 96-well plates at a density of $1 \times 10^5$ cells/mL and incubated for 24 hours. Then, the cells were incubated with the different concentrations of emodin (180, 90, 45, 22.5, 11.25, and 5.625 μM) for 24 hours in 5% $CO_2$ at 37°C. After that, the cells in each well were incubated with 10 μL of 5 mg/mL 3-(4,5)-dimethylthiahiazo (-z-y1)-3,5-di-phenytetrazoliumromide for 3 to 4 hours. Finally, to dissolve the formazan crystals, the cells were incubated with 100 μL of dimethyl sulfoxide with shaking, and the absorbance at 490 nm was measured with a microplate reader (BioTek, Burlington, Vt).

HPDE6-C7 cells in the control group were cultured in regular medium, and those in the STC group were stimulated with STC at a dose of 1016 μM for 1 hour.[16] The cells in the STC + emodin group were pretreated with 5.625, 11.25, 22.5, or 45 μM emodin for 24 hours before being incubated with STC (1016 μM) for 1 hour to analyze the effects of different concentrations of emodin or were pretreated with 45 μM emodin for 3, 6, 12, 24, or 48 hours before being incubated with STC (1016 μM) for 1 hour to analyze the effects of emodin treatment for different durations. Cell viability was determined as described above. Morphological changes in the stimulated cells were visualized with a contrast microscope (Olympus Corp, Tokyo, Japan).

### Quantitative Real-Time Polymerase Chain Reaction

HPDE6-C7 cells were seeded in 6-well plates. The cells in the STC group were treated with STC (1016 μM) for 1 hour, those in the emodin group were treated with 45 μM emodin for 24 hours, and those in the STC + emodin group were pretreated with emodin for 24 hours before being incubated with STC (1016 μM) for 1 hour. Total RNA was extracted from HPDE6-C7 cells subjected to different treatment using the TRIzol Universal Total RNA Extraction Kit following the manufacturer's instructions. To assess RNA integrity, a small amount of total RNA was diluted in RNase-free water, and the absorbance at 260, 280, and 320 nm was measured with a SimpliNano Ultra Micro Spectrophotometer (Biochrom, Cambridge, UK). One microgram of RNA was reverse-transcribed into cDNA with a PrimeScript RT reagent kit on a G-1000 polymerase chain reaction (PCR) system (Bioer Technology, Hangzhou, China). Relative mRNA expression was determined using real-time PCR with SYBR Premix ExTaqTMII (TliRNaseH Plus) on an ABI 7500 Real-Time PCR system (Applied Biosystems, Foster City, Calif). The following conditions were used: amplification at 95°C for 30 seconds, denaturation at 95°C for 5 seconds, and annealing at 60°C for 34 seconds for 40 cycles. The primer sequences are listed in Table 1. The expression levels of all genes were normalized to the expression of β-actin as an endogenous control, and the fold changes among the different groups were calculated by the $2^{-\Delta\Delta CT}$ method for quantitative analysis.

### Flow Cytometry

The percentage of apoptotic cells was determined using an annexin V-FITC/PI apoptosis detection kit. HPDE6-C7 cells were incubated in 6-well plates in different culture media simultaneously. First, HPDE6-C7 cells were digested with 0.25% trypsin, collected in phosphate buffered saline (PBS) and pelleted by centrifugation at 1000 rpm for 5 minutes. Then, the cells collected in binding buffer were stained with 5 μL annexin V-FITC and 5 μL propidium iodide (PI). Finally, the cells were cultured at room temperature away from light for 15 minutes and analyzed by flow cytometry (BD LSRFortessa Cell Analyzer, BD Biosciences, Franklin Lakes, NJ).

Reactive oxygen species generation was assessed using a ROS Detection Assay Kit following the manufacturer's instructions. HPDE6-C7 cells from different groups were collected, and the cell pellets were resuspended in culture medium containing 1 × ROS label. A single-cell suspension was prepared by gently pipetting the cells up and down and incubating them for 30 minutes in the dark. The treated cells were analyzed by flow cytometry (BD LSRFortessa Cell Analyzer, BD Biosciences).

**TABLE 1.** Primer Sequences Used in the Present Work

| Gene | Primers (5′-3′) |
|---|---|
| β-actin | Forward: CCTGGGCATGGAGTCCTGTG |
| | Reverse: TCTTCATTGTGCTGGGTGCC |
| IL-1β | Forward: ATGATGGCTTATTACAGTGGCAA |
| | Reverse: GTCGGAGATTCGTAGCTGGA |
| IL-6 | Forward: AAGCCAGAGCTGTGCAGATGAGTA |
| | Reverse: TGTCCTGCAGCCACTGGTTC |
| IL-8 | Forward: CACTGTGTGTAAACATGACTTCCAA |
| | Reverse: TGTGGTCCACTCTCAATCACTCTC |
| IL-18 | Forward: TCTTCATTGACCAAGGAAATCGG |
| | Reverse: TCCGGGGTGCATTATCTCTAC |


© 2022 The Author(s). Published by Wolters Kluwer Health, Inc.

## Quantification of Total GSH Levels

Total GSH levels were measured with a Micro Reduced GSH Assay Kit according to the manufacturer's instructions. No less than $10^6$ cells from each group were harvested in 1× PBS and collected by centrifugation. Then the cells were suspended by 3 times the volume of protein precipitant to the cell pellet, and the cells underwent freezing-thawing 2 to 3 times. After centrifugation, the supernatant was obtained and placed in a 96-well plate. According to a standard calibration curve, total GSH concentrations were determined using the kinetic method. The absorbance was measured at 412 nm with a microplate reader.

## Measurement of γ-GCS Levels

Levels of γ-GCS were measured according to the instructions of the γ-GCS assay kit. Total protein was extracted from cells in each group with a protein extraction kit. Glutathione promoter was added to the protein samples, and the samples were incubated at 37°C for 6 minutes. Then, the optical density was measured at a wavelength of 636 nm using a microplate reader.

## Animal Experiment

Wild-type male C57BL/6 (20–22 g) mice were provided by the Experimental Animal Center of Dalian Medical University. All animal care and experimental procedures were conducted in accordance with the institutional guidelines for the care and use of laboratory animals and were approved by the Animal Care and Use Committee of Dalian Medical University (no. AEE21019). The mice were anesthetized by isoflurane inhalation. The common hepatic duct was temporarily clamped at the liver hilum to prevent hepatic reflux after a midline incision was made following anesthesia, and 10 μL of 5% STC or 0.9% sodium chloride was then infused into the pancreatic duct for 10 minutes. The catheter and the common hepatic duct clamp were removed after injection. The mice in the emodin and STC + emodin groups were orally administered emodin (75 mg/kg) immediately after animal model establishment and after 6 and 12 hours. The mice in both the control and STC groups were administered an equivalent volume of 1% carboxymethylcellulose sodium at the same time point. The mice were killed 24 hours after AP model establishment, serum was obtained from apical blood samples, 1 part of the pancreas was stored in 4% paraformaldehyde solution, and the remaining part was stored at −80°C.

## Amylase Assay

To evaluate the effects of emodin on AP mice, α-AMS levels in the serum were measured with α-AMS assay kits. Serum samples were diluted 1:100 in PBS, and 100 μL of the final diluted serum was added to substrate buffer in a centrifuge tube. After incubation for 7.5 minutes at 37°C, iodine working solution was added, and the samples were mixed thoroughly. Then, the absorbance at 660 nm was read using a microplate reader.

## Hematoxylin-Eosin Staining

Pancreatic injury was assayed through hematoxylin-eosin (HE) staining. Paraformaldehyde-treated tissue samples were embedded in paraffin wax, and 4-μm tissue sections were cut, dewaxed, rehydrated, and stained with HE. Images of the tissue sections were obtained under a light microscope (Olympus Corp, Tokyo, Japan) at ×200 magnification.

## Western Blotting

Total protein was isolated from HPDE6-C7 cells using a protein extraction kit, and the protein concentration was quantified with a Bicinchoninic Acid protein assay kit. Then, the proteins were separated by sodium dodecyl sulfate-polyacrylamide gel electrophoresis (10%–12%) and transferred onto Polyvinylidene Fluoride membranes (EMD Millipore, Merck KGaA, Darmstadt, Germany). The membranes were incubated overnight at 4°C with primary antibodies against S100A9 (diluted 1:1000 in Tris-buffered saline with Tween) and VNN1 (diluted 1:500 in Tris-buffered saline with Tween). Subsequently, the membranes were incubated with secondary antibodies for 2 hours at room temperature. Finally, protein expression was normalized to that of β-actin, and the protein bands were visualized by enhanced Enhanced Chemiluminescence using a Tanon-5200 Digital Gel Image Analysis System (Tanon Science and Technology Co, Ltd, Shanghai, China). Gel-Pro Analyzer 4.0 software (Media Cybernetics, Rockville, Md) was used for quantitative analysis.

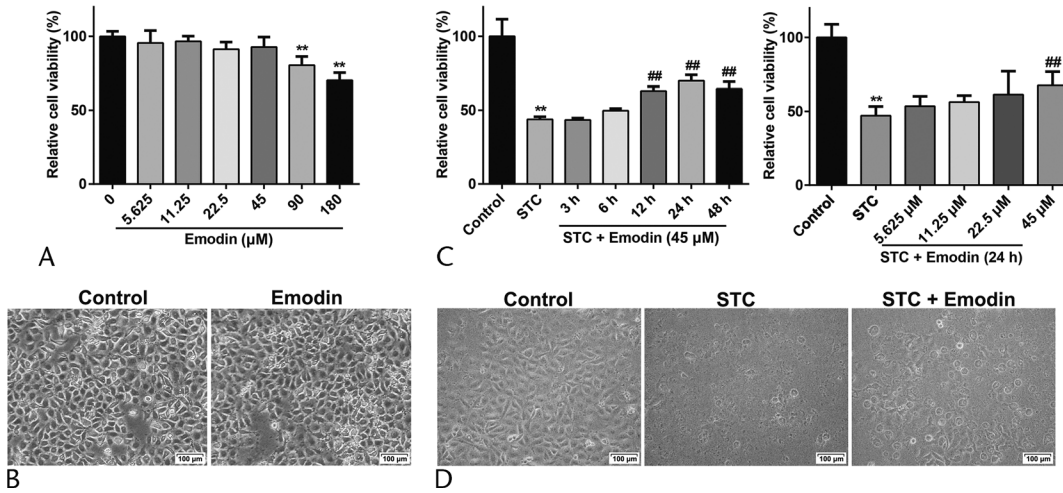


**FIGURE 1.** Emodin alleviated STC-induced HPDE6-C7 cell injury. A, The maximum dose of emodin administered in vitro was 45 μM. N = 6; compared with 0 μM, $^{**}P < 0.01$. B, Emodin had no effect on normal HPDE6-C7 cell morphology. C, The optimal duration of 45 μM emodin treatment in vitro was 24 hours. N = 6. $^{**}P < 0.01$, STC vs control; $^{\#\#}P < 0.01$, emodin + STC vs STC. D, Emodin (45 μM) reversed STC-induced HPDE6-C7 cell morphology damage. Data are expressed as mean ± SEM. Cells were collected 24 hours after STC/emodin treatment.

© 2022 The Author(s). Published by Wolters Kluwer Health, Inc.

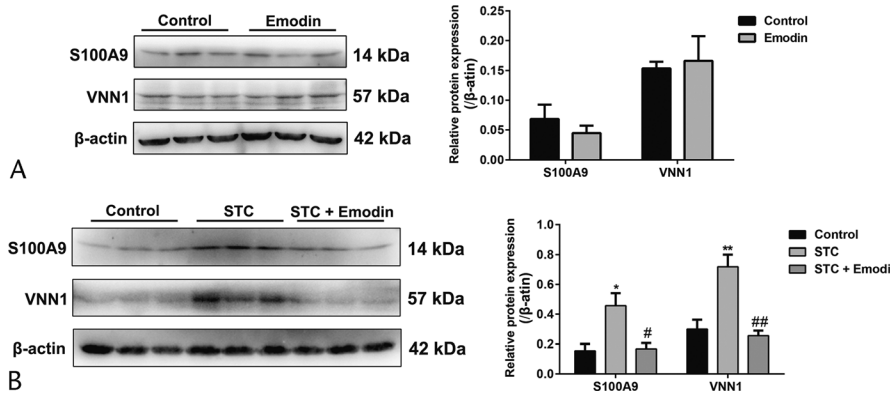


**FIGURE 2.** Emodin regulated S100A9/VNN1 signal–related protein expression in STC-induced HPDE6-C7 cells. A, Both the protein bands and gray value analysis suggested that emodin had no impact on the protein levels of S100A9 and VNN1 in normal HPDE6-C7 cells. B, Emodin reversed the increase in the protein expression of S100A9 and VNN1 induced by STC. Data are expressed as the mean ± SEM. N = 3. $^{*}P < 0.05$ and $^{**}P < 0.01$, STC vs control; $^{\#}P < 0.05$ and $^{\#\#}P < 0.01$, emodin + STC vs STC. Cells were collected 24 hours after STC/emodin treatment.

## Data and Statistical Analysis

The data are presented as the mean ± standard error of the mean (SEM) of at least 3 separate experiments. GraphPad Prism 7.0 software (GraphPad Software, Inc, San Diego, Calif) was used for statistical analysis. One-way analysis of variance followed by Tukey post hoc test (according to homogeneity of variances: yes/no) was used to analyze differences between multiple independent groups. $P < 0.05$ or $< 0.01$ was considered statistically significant.

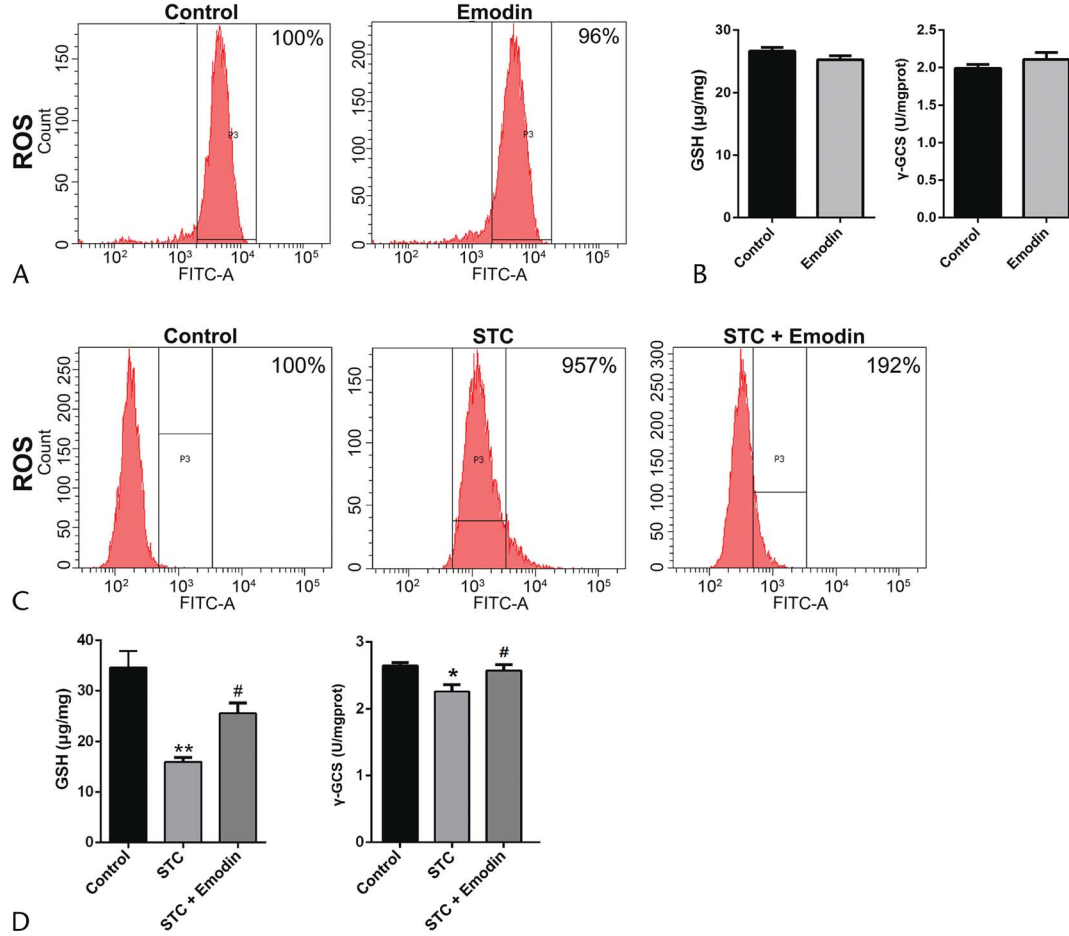


**FIGURE 3.** Emodin inhibited oxidative stress in STC-treated HPDE6-C7 cells. A, Emodin has no effect on ROS levels in normal cells. B, Emodin had no effect on GSH and γ-GCS levels in normal cells. C, The administration of emodin decreased ROS release induced by STC. D, Emodin increased GSH and γ-GCS levels, which were decreased by STC. Data are expressed as mean ± SEM. N = 5. $^{*}P < 0.05$ and $^{**}P < 0.01$, STC vs control; $^{\#}P < 0.05$, emodin + STC vs STC. Cells were collected 24 hours after STC/emodin treatment.


© 2022 The Author(s). Published by Wolters Kluwer Health, Inc.

## RESULTS

### Emodin Alleviated STC-Induced HPDE6-C7 Cell Injury

To identify the dose of emodin that did injure HPDE6-C7 cells, the cytotoxicity of emodin was determined by a cell proliferation assay. Considering the obvious cytotoxicity of 90 μM emodin to HPDE6-C7 cells ($P < 0.01$), the maximum concentration of emodin used in vitro in this study was 45 μM (Fig. 1A). HPDE6-C7 cells were visualized by light microscopy, and no apparent damage to cell morphology was observed in the control or 45 μM emodin treatment group (Fig. 1B). Compared with that of control HPDE6-C7 cells, the viability of HPDE6-C7 cells treated with STC was significantly reduced, but 5.625, 11.25, 22.5, and 45 μM emodin increased cell viability in a dose-dependent manner. Furthermore, use of a time gradient verified that the optimal pretreatment duration for 45 μM emodin was 24 hours (Fig. 1C). Analysis of cell morphology showed that STC-stimulated HPDE6-C7 cells were mainly round and bright and that STC increased the number of dead HPDE6-C7 cells and decreased the total HPDE6-C7 cell number, whereas emodin (45 μM) reversed STC-induced HPDE6-C7 cell damage (Fig. 1D).

### Emodin Regulated the Expression of S100A9/VNN1 Signaling–Related Proteins in STC-Stimulated HPDE6-C7 Cells

As shown in Figure 2A, emodin had no impact on the protein levels of S100A9 and VNN1 in normal HPDE6-C7 cells. The protein expression levels of S100A9 and VNN1 were notably increased after the addition of STC, whereas emodin reversed the increase in the protein expression of S100A9 and VNN1 induced by STC, as shown in Figure 5B, suggesting that emodin alleviates STC-induced HPDE6-C7 cell injury by inhibiting the S100A9/VNN1 signaling pathway.

### Emodin Inhibited Oxidative Stress in STC-Treated HPDE6-C7 Cells

The levels of ROS, GSH, and γ-GCS were not significantly changed in the emodin treatment group compared with the control group (Figs. 3A, B). The ROS levels in the STC group were significantly increased compared with those in the control group, and after the administration of emodin, ROS levels were obviously decreased (Fig. 3C). In contrast, GSH and γ-GCS levels were decreased by STC, but increased by emodin (Fig. 3D). These results indicated that inhibition of S100A9/VNN1 signaling by emodin can restore redox homeostasis in STC-stimulated HPDE6-C7 cells.

### Emodin Reversed STC-Induced Apoptosis of HPDE6-C7 Cells

Apoptosis of HPDE6-C7 cells was analyzed by FITC Annexin V-PI double labeling and flow cytometry. Cell apoptosis was not affected by treatment with 45 μM emodin, as shown in Figure 4A. As shown in Figure 4B, apoptosis of HPDE6-C7 cells was promoted in the STC stimulation group compared with the control group, and emodin treatment inhibited the induction of apoptosis by STC. The relative apoptosis rate after emodin treatment was higher than that in the control group but lower than that in the STC stimulation group. These results indicated that inhibition of S100A9/VNN1 signaling by emodin may alleviate STC-induced HPDE6-C7 cell apoptosis.

### Emodin Reduced Inflammatory Factor Release From STC-Stimulated HPDE6-C7 Cells

We explored the effects of emodin on the expression of inflammatory factors in STC-stimulated HPDE6-C7 cells. Compared with those in the control group, the mRNA levels of interleukin (IL)-1β, IL-6, and IL-8 in the emodin treatment group were significantly decreased, whereas there were no significant changes in IL-18 mRNA levels after emodin treatment (Fig. 5A). The mRNA levels of IL-1β, IL-6, IL-8, and IL-18 in the STC group were significantly higher than those in the control group; however,

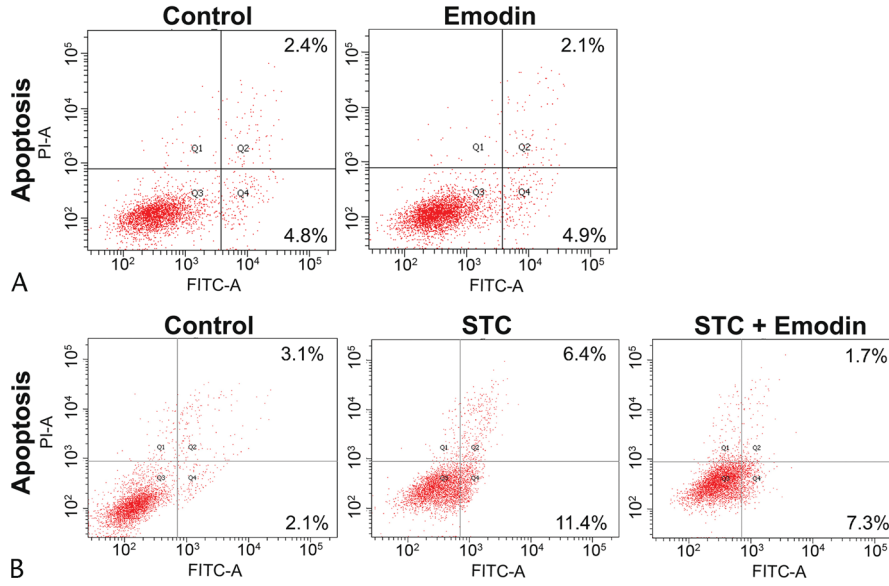


**FIGURE 4.** Emodin reversed STC-induced apoptosis of HPDE6-C7 cells. A, Emodin did not promote or inhibit normal cell apoptosis. B, Apoptosis of HPDE6-C7 cells following STC stimulation could be repressed by emodin treatment. Cells were collected 24 hours after STC/emodin treatment.

© 2022 The Author(s). Published by Wolters Kluwer Health, Inc.

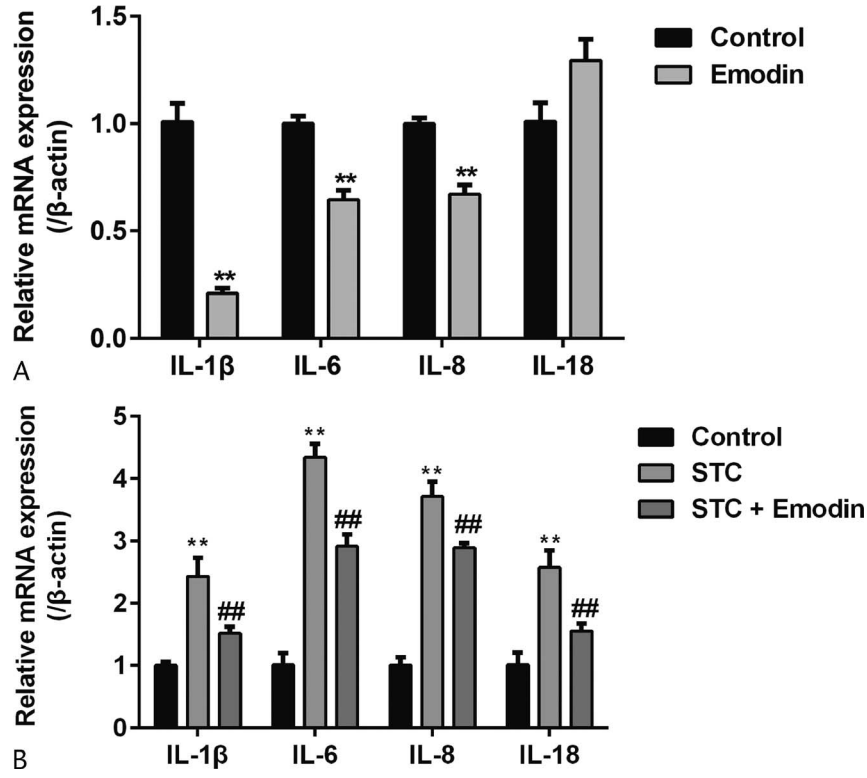


**FIGURE 5.** Emodin reduced the release of inflammatory factors from STC-damaged HPDE6-C7 cells. A, Emodin significantly reduced IL-1β, IL-6, and IL-8 levels without affecting IL-18 levels. B, Emodin reduced the massive release of the inflammatory factors IL-1β, IL-6, IL-8, and IL-18 by HPDE6-C7 cells induced by STC. Data are expressed as mean ± SEM. N = 3. $^{**}P < 0.01$, STC vs control; $^{\#\#}P < 0.01$, emodin + STC vs STC. Cells were collected 24 hours after STC/emodin treatment.

the expression levels of these factors in the STC + emodin (45 μM) group were lower than those in the STC group (Fig. 5B). These results indicated that blockade of the S100A9/VNN1 pathway by emodin can reduce the massive release of inflammatory factors caused by STC.

## Emodin Relieved STC-Induced AP in Mice

As shown in Figure 6A, compared with those in mice exposed to STC, serum α-AMS levels in mice treated with emodin were significantly decreased. The protein levels of S100A9 and

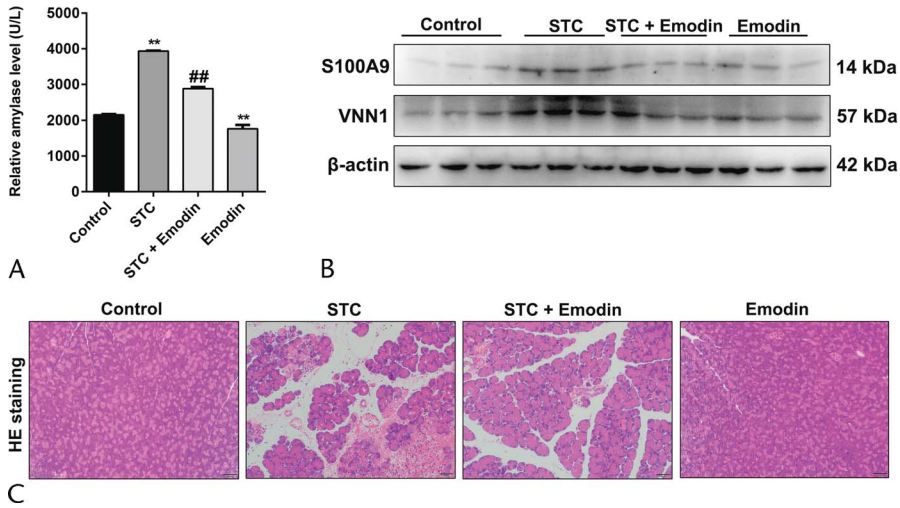


**FIGURE 6.** Emodin relieved STC-induced AP in mice. A, Emodin reduced serum amylase levels in mice with STC-induced AP. Data are expressed as mean ± SEM. N = 6. $^{**}P < 0.01$, STC vs control, and emodin vs control; $^{\#\#}P < 0.01$, emodin + STC vs STC. B, Emodin inhibited the protein expression of S100A9 and VNN1 in the pancreas in mice with STC-induced AP. N = 3. C, Emodin relieved pancreatic damage in mice with STC-induced AP.


© 2022 The Author(s). Published by Wolters Kluwer Health, Inc.

VNN1 in the STC group were obviously higher than those in the control group; however, the expression levels of these proteins in the emodin (45 μM) group were lower than those in the STC group (Fig. 6B). In addition, HE staining showed obvious pancreatic damage, including vacuolization, increased neutrophils, and a small amount of bleeding, in mice treated with STC; however, these deleterious changes were significantly ameliorated by emodin. Moreover, emodin had no effect on the pancreatic tissue of normal mice (Fig. 6C). These results indicated that emodin can alleviate the STC-induced AP in mice by repressing the S100A9/VNN1 pathway.

## DISCUSSION

At present, because most studies on AP have focused on physiological changes in pancreatic acinar cells, efforts to identify the drugs for AP are focused mainly on acinar cell injury.[24,26] Interestingly, pancreatic ductal cells, as one of the main components of the exocrine pancreas, also play an important role in maintaining the physiological function of the pancreas.[27] Our previous study revealed that pancreatic ductal cells are the first to be exposed to the toxic stimuli related to pancreatitis, which indirectly lead to structural and functional impairment of pancreatic acinar cells.[16] Although many previous studies have confirmed that TCM compounds, Chinese herbs, and natural products have effects against AP, the mechanisms of action of TCM compounds against AP is still unclear.[17,20,24] The compositions of TCM compounds are complex and diverse; each Chinese herb has its own characteristics and different processing and compatibility methods lead to different curative effects.[28] Much effort is needed to determine the drug compositions and pharmacological characteristics of TCM compounds, and such investigations are tedious. Based on previous clinical and experimental research, the efficacy of TCM formulas, such as Dachengqi decoction and Qingyi decoction, in the treatment of AP has been confirmed.[18,29] As the key ingredients of these 2 decoctions, the active components of rhubarb have been successfully isolated and identified.[30] Emodin is one of the main active components of rhubarb. Our previous studies confirmed that emodin alleviates STC-induced pancreatic acinar cell injury and inflammation, as well as adenosine triphosphate-stimulated pancreatic duct cell injury.[24,25] In this study, we established a model of STC-stimulated HPDE6-C7 cell injury to explore whether emodin has a protective effect against pancreatic duct injury in vitro and its potential mechanisms. The results showed that the viability and morphology of STC-stimulated HPDE6-C7 cells treated with 45 μM emodin for 24 hours were significantly improved.

The calcium-binding protein S100A9 is abundantly expressed in monocytes-macrophages and neutrophils, and it is also located in the cytoplasm and plasma membrane of pancreatic cells under normal conditions in the human gastrointestinal system.[31] S100A9 is rapidly released upon necrosis or actively secreted by damaged cells and acts as a damage-associated molecular pattern in response to inflammatory stimuli.[32] S100A9 selectively binds to $Ca^{2+}$, $Zn^{2+}$, arachidonic acid, as well as receptor for advanced glycation end products and toll-like receptor 4, with strong affinity and has intracellular and extracellular regulatory effects associated with the inflammatory response and tumorigenesis.[33] Shen et al[34] found that plasma S100A9 levels in patients with acute ischemic stroke can be used as biomarkers for the therapeutic evaluation of 4 TCM formulations (Buyang Huanwu decoction, Xuefu Zhuyu decoction, Tianma Gouteng decoction, and Shengyu decoction) before functional recovery can be observed. However, to date, there is no related research on the efficacy of rhubarb and its active component emodin in the treatment of AP via regulation of S100A9 expression. In our previous study based on isobaric tags for relative and absolute quantitation proteomics, we found that the expression of S100A9 in the pancreatic tissues of rats with AP was significantly increased.[35] Mechanistically, S100A9, as a key regulator of STC-induced pancreatic duct cell injury, may activate the PYD domain–containing protein 3 inflammasome and aggravate AP through VNN-mediated ROS release.[16] VNN1 is a glycosylated phosphatidylinositol-anchored extracellular enzyme that can hydrolyze pantothenate into pantothenic acid and cysteamine, thereby inhibiting γ-GCS enzyme activity and GSH activity. Previous studies have evaluated the function of VNN1 in oxidative stress, showing that upregulation of VNN1 expression can lead to activation of the proinflammatory response in the microenvironment by reducing antioxidant activity.[36,37] In this work, we explored the function of S100A9 as a potential target of emodin in the treatment of AP for the first time. By measuring the protein expression of S100A9 and VNN1, we found that emodin can effectively inhibit the S100A9/VNN1 signaling pathway in STC-treated HPDE6-C7 cells and reduce the mass release of ROS. We also measured GSH and γ-GCS activity in HPDE6-C7 cells and found that GSH levels and γ-GCS enzyme activity were significantly increased by emodin-mediated inhibition of the S100A9/VNN1 pathway.

Generally, emodin can significantly inhibit the expression of S100A9 in HPDE6-C7 cells stimulated with STC, thus inhibiting the release of ROS mediated by VNN1, increasing antioxidant activity in injured duct cells, inhibiting the inflammatory cascade and ameliorating pancreatic duct injury in AP. Therefore, S100A9 may be an important target of emodin in the treatment of AP.

## REFERENCES


1. Goodman RR, Jong MK, Davies JE. Concise review: the challenges and opportunities of employing mesenchymal stromal cells in the treatment of acute pancreatitis. *Biotechnol Adv*. 2020;42:107338.
2. Lankisch PG, Apte M, Banks PA. Acute pancreatitis. *Lancet*. 2015;386: 85–96.
3. Párniczky A, Kui B, Szentesi A, et al. Prospective, multicentre, nationwide clinical data from 600 cases of acute pancreatitis. *PLoS One*. 2016; 11:e0165309.
4. Lee PJ, Papachristou GI. New insights into acute pancreatitis. *Nat Rev Gastroenterol Hepatol*. 2019;16:479–496.
5. Habtezion A, Gukovskaya AS, Pandol SJ. Acute pancreatitis: a multifaceted set of organelle and cellular interactions. *Gastroenterology*. 2019;156:1941–1950.
6. Wang Q, Bai L, Luo S, et al. TMEM16A $Ca^{2+}$-activated $Cl^-$ channel inhibition ameliorates acute pancreatitis via the $IP_3R/Ca^{2+}$/NFκB/IL-6 signaling pathway. *J Adv Res*. 2020;23:25–35.
7. Wen L, Voronina S, Javed MA, et al. Inhibitors of ORAI1 prevent cytosolic calcium-associated injury of human pancreatic acinar cells and acute pancreatitis in 3 mouse models. *Gastroenterology*. 2015;149:481–492.e7.
8. Duan PY, Ma Y, Li XN, et al. Inhibition of RIPK1-dependent regulated acinar cell necrosis provides protection against acute pancreatitis via the RIPK1/NF-κB/AQP8 pathway. *Exp Mol Med*. 2019;51:1–17.
9. Pallagi P, Hegyi P, Rakonczay Z Jr.The physiology and pathophysiology of pancreatic ductal secretion: the background for clinicians. *Pancreas*. 2015; 44:1211–1233.
10. Venglovecz V, Rakonczay Z, Ozsvári B, et al. Effects of bile acids on pancreatic ductal bicarbonate secretion in guinea pig. *Gut*. 2008;57: 1102–1112.
11. Maléth J, Venglovecz V, Rázga Z, et al. Non-conjugated chenodeoxycholate induces severe mitochondrial damage and inhibits bicarbonate transport in pancreatic duct cells. *Gut*. 2011;60:136–138.
12. Leung PS. Physiology of the pancreas. *Adv Exp Med Biol*. 2010;690: 13–27.


© 2022 The Author(s). Published by Wolters Kluwer Health, Inc.

13. Lightner AM, Kirkwood KS. Pathophysiology of gallstone pancreatitis. *Front Biosci*. 2001;6:E66–E76.

14. Uomo G, Molino D, Visconti M, et al. The incidence of main pancreatic duct disruption in severe biliary pancreatitis. *Am J Surg*. 1998;176: 49–52.

15. Schnekenburger J, Schick V, Krüger B, et al. The calcium binding protein S100A9 is essential for pancreatic leukocyte infiltration and induces disruption of cell-cell contacts. *J Cell Physiol*. 2008;216:558–567.

16. Xiang H, Guo F, Tao X, et al. Pancreatic ductal deletion of S100A9 alleviates acute pancreatitis by targeting VNN1-mediated ROS release to inhibit NLRP3 activation. *Theranostics*. 2021;11:4467–4482.

17. Hu J, Li P, Zhang T. Rhubarb combined with trypsin inhibitor for severe acute pancreatitis: a systematic review and meta-analysis. *Phytother Res*. 2018;32:1450–1458.

18. Zhang JW, Zhang GX, Chen HL, et al. Therapeutic effect of Qingyi decoction in severe acute pancreatitis-induced intestinal barrier injury. *World J Gastroenterol*. 2015;21:3537–3546.

19. Sun W, Chen Y, Li H, et al. Material basis and molecular mechanisms of Dachengqi decoction in the treatment of acute pancreatitis based on network pharmacology. *Biomed Pharmacother*. 2020;121:109656.

20. Xiang H, Wang G, Qu J, et al. Yin-Chen-Hao Tang attenuates severe acute pancreatitis in rat: an experimental verification of *in silico* network target prediction. *Front Pharmacol*. 2016;7:378.

21. Xia S, Ni Y, Zhou Q, et al. Emodin attenuates severe acute pancreatitis via antioxidant and anti-inflammatory activity. *Inflammation*. 2019;42: 2129–2138.

22. Ni Q, Sun K, Chen G, et al. In vitro effects of emodin on peritoneal macrophages that express membrane-bound CD14 protein in a rat model of severe acute pancreatitis/systemic inflammatory response syndrome. *Mol Med Rep*. 2014;9:355–359.

23. Li J, Zhou R, Bie BB, et al. Emodin and baicalein inhibit sodium taurocholate–induced vacuole formation in pancreatic acinar cells. *World J Gastroenterol*. 2018;24:35–45.

24. Xiang H, Tao X, Xia S, et al. Emodin alleviates sodium taurocholate–induced pancreatic acinar cell injury via microRNA-30a-5p-mediated inhibition of high-temperature requirement A/transforming growth factor beta 1 inflammatory signaling. *Front Immunol*. 2017;8:1488.

25. Zhang Q, Hu F, Guo F, et al. Emodin attenuates adenosine triphosphate-induced pancreatic ductal cell injury in vitro via the inhibition of the P2X7/NLRP3 signaling pathway. *Oncol Rep*. 2019;42:1589–1597.

26. Sebai H, Ristorcelli E, Sbarra V, et al. Protective effect of resveratrol against LPS-induced extracellular lipoperoxidation in AR42J cells partly via a Myd88-dependent signaling pathway. *Arch Biochem Biophys*. 2010;495: 56–61.

27. Pallagi P, Balla Z, Singh AK, et al. The role of pancreatic ductal secretion in protection against acute pancreatitis in mice*. *Crit Care Med*. 2014;42: e177–e188.

28. Normile D. Asian medicine. The new face of traditional Chinese medicine. *Science*. 2003;299:188–190.

29. Zhang YM, Zhu L, Zhao XL, et al. Optimal timing for the oral administration of Da-Cheng-Qi decoction based on the pharmacokinetic and pharmacodynamic targeting of the pancreas in rats with acute pancreatitis. *World J Gastroenterol*. 2017;23:7098–7109.

30. Xiang H, Zuo J, Guo F, et al. What we already know about rhubarb: a comprehensive review. *Chin Med*. 2020;15:88.

31. Pruenster M, Vogl T, Roth J, et al. S100A8/A9: from basic science to clinical application. *Pharmacol Ther*. 2016;167:120–131.

32. Lim SY, Raftery MJ, Geczy CL. Oxidative modifications of DAMPs suppress inflammation: the case for S100A8 and S100A9. *Antioxid Redox Signal*. 2011;15:2235–2248.

33. Markowitz J, Carson WE 3rd. Review of S100A9 biology and its role in cancer. *Biochim Biophys Acta*. 2013;1835:100–109.

34. Shen YC, Lu CK, Liou KT, et al. Common and unique mechanisms of Chinese herbal remedies on ischemic stroke mice revealed by transcriptome analyses. *J Ethnopharmacol*. 2015;173:370–382.

35. Xiang H, Zhang Q, Wang D, et al. iTRAQ-based quantitative proteomic analysis for identification of biomarkers associated with emodin against severe acute pancreatitis in rats. *RSC Adv*. 2016;6:72447–72457.

36. Kang M, Qin W, Buya M, et al. VNN1, a potential biomarker for pancreatic cancer-associated new-onset diabetes, aggravates paraneoplastic islet dysfunction by increasing oxidative stress. *Cancer Lett*. 2016;373: 241–250.

37. Naquet P, Pitari G, Duprè S, et al. Role of the Vnn1 pantetheinase in tissue tolerance to stress. *Biochem Soc Trans*. 2014;42:1094–1100.


© 2022 The Author(s). Published by Wolters Kluwer Health, Inc.